DOI: 10.17725/j.rensit.2024.16.137

The grid-characteristic method on chimeric meshes application to study the keel morphometric characteristics of ice ridges

Evgeniy A. Pesnya, Maxim V. Muratov, Alena V. Favorskaya, Anton A. Kozhemyachenko

Moscow Institute of Physics and Technology, https://mipt.ru/

Dolgoprudny 141700, Moscow region, Russian Federation

E-mail: pesnya.ea@phystech.edu, max.muratov@gmail.com, aleanera@yandex.ru, kozhemyachenko@yandex.ru

Received November 24, 2023, peer-reviewed November 30, 2023, accepted December 07, 2023, published March 15, 2024.

Abstract: **Designing engineering structures in the Arctic zone requires to consider the loads transmitted to the structure construction in connection with collisions with various ice formations: icebergs, ice ridges, stamukhs. The paper considers the use of the grid-characteristic method for modeling the passage of elastic waves in a cross-section of the ice ridge together with its porosity in the consolidated layer and in the lower part of the keel. We propose to use chimeric (overlapped) computational meshes for the describing curvilinear shape of pores filled with air or water. As a result of computer simulation, the direct problem of ultrasound investigation of the ice ridge has solved, velocity vector fields have obtained at various moments in time, including a system of reflections from pores.**

Keywords: **computer simulation, grid-characteristic method, ice ridges morphometry, ultrasound investigation**

UDC 519.63

Acknowledgments: This work was carried out with the financial support of the Russian Science Foundation, project no. 21-71-10015.

For citation: Engeniy A. Pesnya, Maxim V. Muratov, Alena V. Favorskaya, Anton A. Kozhemyachenko. The grid-characteristic method on chimeric meshes application to study the keel morphometric characteristics of ice ridges. *RENSIT: Radioelectronics. Nanosystems. Information Technologies,* 2024, 16(2):137-142e. DOI: 10.17725/j.rensit.2024.16.137.

Contents

1. Introduction (137)
2. Materials and methods (138)
3. Results and discussion (140)
4. Conclusion (140)

References (141)

1. INTRODUCTION

The safety of the operation of oil-producing facilities and shipping in the Arctic regions is affected by loads when interacting with hummocks. To obtain design estimates of ice loads on engineering structures, it is necessary to conduct a morphometric analysis of the characteristics of such ice formations. Ice ridges formed as a result of compression of the ice sheet are called a hummock, while the surface part of the hummock is called a sail, and the underwater part is called a keel. For example, [1-2] provide information on the morphometry and internal structure of the hummock of the first year of formation using electrothermal drilling in the Barneo ice camp. At the same time, it is customary to use sonar approaches to study the lower part of the hummocks [3]. A large set of statistical data on ice sediment and keel depth collected by upward-pointing sonars is given in [4] for five locations in the Barents Sea. Another morphometric analysis of the keel of hummocks of the first year of formation using sonar has performed in [5], where it has assumed that the best generalization of the shape of the ridges of the first year is the trapezoidal shape of the keel. In [6] the keels of hummocks have been monitored using sonar located on the bridge in the Northumberland Strait. The shape of the keels has been classified as one of four shapes: triangular, trapezoidal, w-shaped and keels with multiple peaks. The observed distributions of keel depth values have been compared with the calculated ones. In [7] the ice sheet and the ice ridge are modeled as thin elastic plates to consider the interaction of waves with the round body trapped by a thin layer of sea ice, an analytical analysis of the impact of waves on a circular ice ridge embedded in the ice sheet is conducted. In [8-9] the probabilistic method based on the search for the relationship between the levels of ice precipitation, the sediment of the keel of the hummock and the frequency of ridge formation is proposed to assess the loads transmitted to offshore structures. The analysis of seasonal data obtained with the help of sonar in the Beaufort Sea on the levels of ice precipitation, the keel of the ice ridge, the frequency of ridge formation allowed us to obtain probabilistic analytical approaches for modeling the age of the ridge, determining the formula for the growth of the consolidated layer and studying its thickness. Based on a field experiment on strengthening the artificial ice ridge in [10] analytical and two-dimensional discrete numerical modeling approaches have been obtained to predict the thickness of the consolidated layer in the probabilistic analysis of the impact of ice on structures that require information about meteorological conditions and general physical and mechanical properties of ice as input data. At the same time, numerical modeling of the ice level and ridge consolidation has been performed using the finite element method, and the position of the ice-water boundary has been determined from the Stefan energy balance condition.

In [11] to study the structure of ice ridges of various configurations, the grid-characteristic method is used on structured regular computational meshes and the comparative analysis of the seismograms obtained using full-wave modeling is conducted. To solve the equations of mathematical physics, chimeric or overlapping computational meshes have recently been used, which are previously used to solve hydrodynamic problems [12-13]. The grid-characteristic method using chimeric meshes makes it possible to describe the boundaries of a complex shape [14-15], including contact [16] or non-aligned with coordinate axes [17-19]. In this paper to describe curved cavities filled with air or water, the grid-characteristic method is used with chimeric regular computational meshes.

2. MODELS AND METHODS

For numerical simulation of the problem of wave signal propagation in the hummock systems of equations for an isotropic linear elastic medium and for an acoustic medium are jointly considered, which in general can be reduced to the following system of equations:

$$\frac{\partial \mathbf{u}}{\partial t} + \mathbf{A}_1 \frac{\partial \mathbf{u}}{\partial x} + \mathbf{A}_2 \frac{\partial \mathbf{u}}{\partial y} = 0, \tag{1}$$

where in (1) $\mathbf{u}$ – vector of the unknown functions.

In the case of the linear elastic medium, the vector of the unknown functions are considered $\mathbf{u} = (v_x, v_y, \sigma_{xx}, \sigma_{yy}, \sigma_{xy})^T$, that is the components of the perturbation propagation velocity **v** and the components of the symmetric Cauchy stress tensor **σ**. Matrices $\mathbf{A}_1$, $\mathbf{A}_2$ have the set of eigenvalues $\{c_P, -c_P, c_s, -c_s, 0\}$, where c_p – the velocity of propagation of longitudinal waves, c_s – the velocity of propagation of transverse waves.

In the case of the acoustic medium the unknown functions are $\mathbf{u} = (v_x, v_y, p)^T$, that is the components of the perturbation propagation velocity **v** and pressure *p*. Matrices have the set of eigenvalues $\{c_P, -c_P, 0\}$.

Thus, the systems of equations (1), describing a linearly elastic body and an acoustic medium are hyperbolic, which means that in both cases the matrices $\mathbf{A}_1$, $\mathbf{A}_2$ can be represented as

$$\mathbf{A} = \mathbf{\Omega\Lambda\Omega}^{-1},$$

where the matrix $\mathbf{\Omega}$ consists of columns that are the right eigenvectors of the original matrix, which, in turn, correspond to the eigenvalues, which are elements of the diagonal matrix $\mathbf{\Lambda}$. Splitting the system (1) in spatial directions, we proceed to the Riemann invariants $\boldsymbol{\omega}\mathbf{\Omega}^{-1}\mathbf{u}$, which are transferred according to the characteristics of the hyperbolic system, we obtain the hyperbolic system from linear transfer equations with constant coefficients in Riemann invariants

$$\frac{\partial \boldsymbol{\omega}}{\partial t} + \mathbf{\Lambda}\frac{\partial \boldsymbol{\omega}}{\partial x} = 0. \qquad (2)$$

The system in Riemann invariants (2) on the upper layer in time can be numerically integrated using finite-difference schemes, for example, using the Rusanov scheme of the third order in time and space [16], used in calculations in this paper. To move to the components $\mathbf{v}$ and $\boldsymbol{\sigma}$ or $\mathbf{v}$ and p respectively on the upper layer in time after calculating the Riemann invariants, the inverse transformation is used $\mathbf{u} = \mathbf{\Omega}\boldsymbol{\omega}$.

The basic model of the ice ridge is shown in **Fig. 1**, where the red cross section schematically shows the calculated area when considering the lower part of the keel of the hummock. **Fig. 2***a* and Fig. 2*b* show the calculated areas of 16 by 16 meters, in which seismic responses from cavities and pores filled with air or water are studied for the case of specifying the source in the consolidated layer of the hummock and in

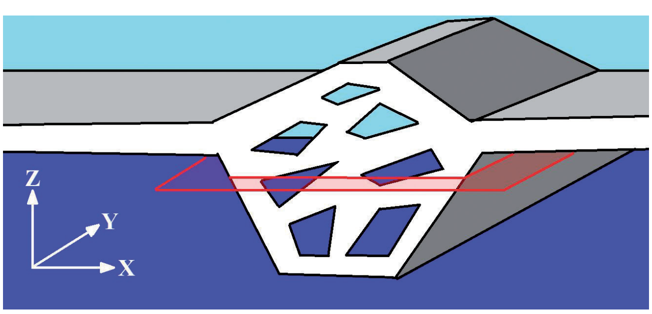

Fig. 1. *The basic model of the ice ridge (hummock).*

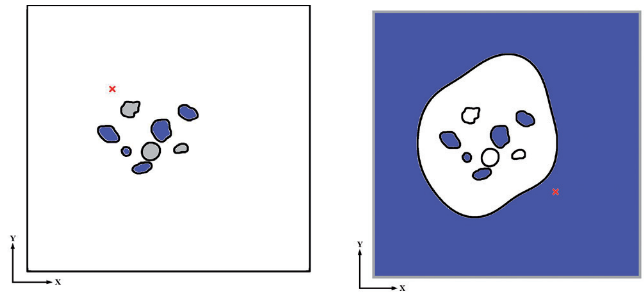

a *b*

Fig. 2. *The cross section of the ice ridge with cavities filled with air (gray areas) or water (blue areas): a – in the consolidated layer, b – in the lower part of the keel.*

Table 1

Parameters of simulated media

medium	Velocity P-wave, m/s	Velocity S-wave, m/s	Density, kg/m³
Ice	3940	2493	917
Water	1500	–	1000

the seawater, when considering the lower part of the keel, respectively. The characteristics of the media are given in **Table 1**. It is worth noting that by changing the corresponding parameters of the medium (velocity, density), ice formations with different salinity and temperature conditions can be considered.

At the boundaries of the ice-air interface the conditions of the free border were set

$$\boldsymbol{\sigma}\cdot\mathbf{n} = 0,$$

where $\mathbf{n}$ – normal to the corresponding boundary.

At the interface of the ice-water media (1 and 2 media respectively) the following contact condition was set:

$$\mathbf{v}_1\cdot\mathbf{n} = \mathbf{v}_2\cdot\mathbf{n},$$
$$\boldsymbol{\sigma}_1\cdot\mathbf{n} + p\cdot\mathbf{n} = 0,$$

here $\mathbf{n}$ – normal to the boundary of the contacting medium 1.

Non-reflecting boundary conditions are used at the boundaries of the computational domain in Fig. 2. The Riker impulse with the frequency of 25 kHz was used as the initial perturbation, the source location is marked in Fig. 2 with a red cross.

In the calculation the integration areas in Fig. 2 were covered with background rectangular computational grids and curved chimeric meshes with the characteristic spatial step of 10^{-2} m, the integration step in time was $2.54\cdot10^{-7}$ s. The

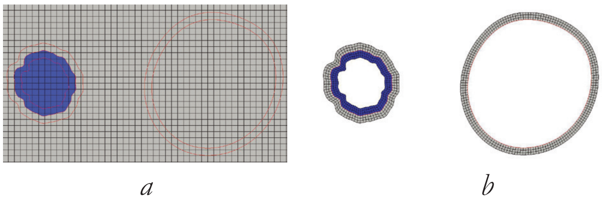

Fig. 3. *The example of the configuration of computational meshes: a – background mesh, b – chimeric meshes.*

example of the location of the background and overlapped meshes for cavities filled with air and water is shown in **Fig. 3.** The nodes of the background mesh contain information about the parameters of the medium, so in Fig. 3*a* ice is highlighted in gray, water is highlighted in blue. At the same time, to describe the cavities in the boundary region, the calculation was performed using overlapped meshes according to Fig. 3*b*, which, considering the boundary conditions and the mutual interpolation algorithm [18], allows correctly calculate the wave signal propagation through water pores and does not consider the areas filled with air in the calculation.

3. RESULTS AND DISCUSSION

Fig. 4 and **Fig. 5** show the results of full-wave modeling of the propagation of perturbation and wave responses from the cavities under

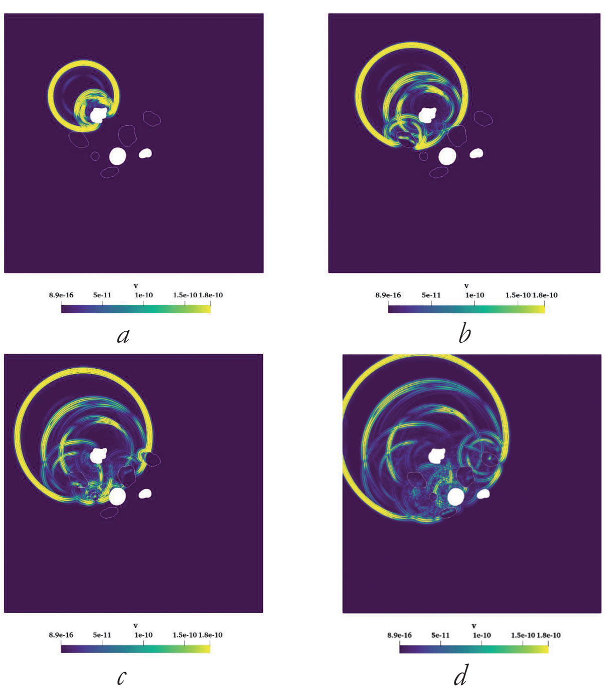

Fig. 4. *Propagation of wave responses from the system of cavities in a slice located in the consolidated layer: a – 0.014 s, b – 0.021 s, c – 0.027 s, d – 0.034 s.*

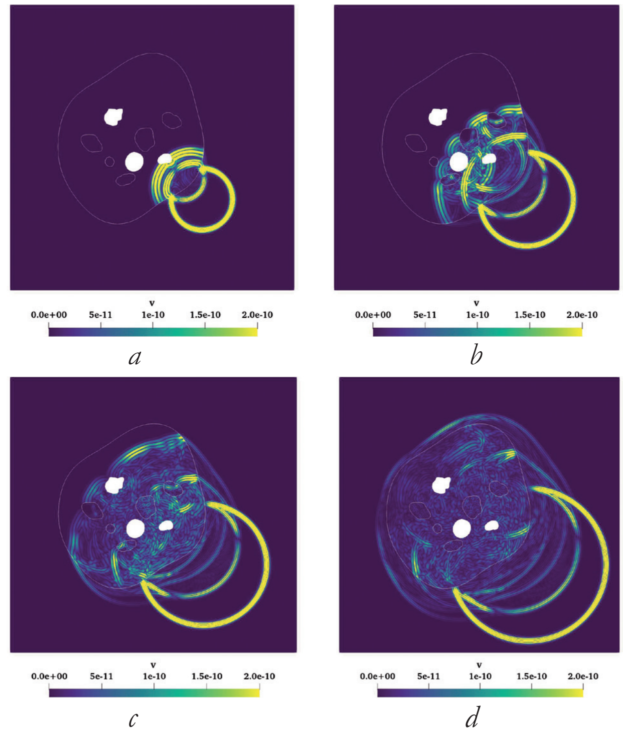

Fig. 5. *Propagation of wave responses from a system of cavities in the slice located in the lower part of the keel: a – 0.030 s, b – 0.045 s, c – 0.060 s, d –0.075 s.*

consideration at various points in time when considering the computational domain in the consolidated layer of the hummock and the lower part of its keel, respectively.

In Fig. 4*a* the first response is formed from a cavity filled with air, in Fig. 4*b* the initial impulse is reflected from the pore filled with water, while part of the wavefront passes through the pore. Fig. 4*c* and Fig. 4*d* show the complex system of reflections from all remaining pores and cavities.

In Fig. 5*a* the first reflections occur from the keel of the hummock itself and the first cavity in the future, new reflected signals from other cavities are formed, incoming from the ice surface of the keel into the water in Fig. 5*b* and Fig. 5*c*, and in Fig. 5*d* the original signal completely passes the thickness of the keel.

4. CONCLUSION

Using the grid-characteristic method on structured rectangular and chimeric regular computational meshes, the direct problem of the passage of the ultrasonic signal along the hummock is solved and the results of full-wave modeling of the velocity vector at various points in time are obtained. The proposed approach allows consider the complex geometry and structure, porosity of the ice ridge. The obtained algorithms and models can be used to obtain and analyse synthetic seismograms, which can be used to determine a number of morphometric parameters of the hummock, when solving the inverse problem.

REFERENCES

1. Kharitonov VV. Morphometry and unusual internal structure of ice ridge investigated at Barneo ice camp in April 2013. Polar Science, 2022, 31:100736.
2. Kharitonov VV, Borodkin VA. On the results of studying ice ridges in the Shoka-l'skogo Strait, part I: Morphology and physical parameters in-situ. Cold Regions Science and Technology, 2020, 174:103041.
3. Mironov YU, Guzenko RB, Porubaev VS, Kharitonov VV, Khotchenkov SV and Nesterov AV. Morphometric Parameters of Stamukhas in the Laptev Sea. International Journal of Offshore and Polar Engineering, 2019, 29(4):383-390.
4. Hansen E, Ervik Å, Eik K, Olsson A, Teigen SH. Long-term observations (2014–2020) of level ice draft, keel depth and ridge frequency in the Barents Sea. Cold Regions Science and Technology, 2023, 216:103988.
5. Ekeberg O, Høyland K, Hansen E. Ice ridge keel geometry and shape derived from one year of upward looking sonar data in the Fram Strait. Cold Regions Science and Technology, 2015, 109:78-86.
6. Obert KM, Brown TG. Ice ridge keel characteristics and distribution in the Northumberland Strait. Cold Regions Science and Technology, 2011, 66(2-3):53-64.
7. Mandal S, Law AW, Shen HH. Wave interactions with circular ice ridge embedded in level ice. Cold Regions Science and Technology, 2018, 155:90-99.
8. Samardžija I, Høyland K, Leira BJ, Naess A. Consolidated layer thickness in probabilistic simulation of first-year ice ridges. Cold Regions Science and Technology, 2023, 216:104021.
9. Samardžija I, Høyland K. Analysis of the relationship between level ice draft, ridge frequency and ridge keel draft for use in the probabilistic assessment of ice ridge loads on offshore structures. Ocean Engineering, 2023, 270:113593.
10. Salganik E, Høyland K, Shestov A. Medium-scale experiment in consolidation of an artificial sea ice ridge in Van Mijenfjorden, Svalbard. Cold Regions Science and Technology, 2021, 181:103194.
11. Favorskaya AV, Muratov MV. Ultrasonic Study of Sea Ice Ridges. In: Czarnowski, I., Howlett, R.J., Jain, L.C. (eds) Intelligent Decision Technologies. Smart Innovation, Systems and Technologies, 2022, 309, Springer, Singapore.
12. Henshaw WD, Schwendeman DW. Parallel computation of three-dimensional flows using overlapping grids with adaptive mesh refinement. Journal of Computational Physics, 2008, 227(16):7469-7502.
13. Chang XH, Ma R, Wang NH, Zhao Z, Zhang LP. A Parallel Implicit Hole-cutting Method Based on Background Mesh for Unstructured Chimera Grid. Computers & Fluids, 2020, 198:104403.
14. Favorskaya AV, Khokhlov NI, Petrov IB. Grid-Characteristic Method on Joint Structured Regular and Curved Grids for Modeling Coupled Elastic and Acoustic Wave Phenomena in Objects of Complex Shape. Lobachevskii Journal of Mathematics, 2020. 41(4):512-525.
15. Kozhemyachenko A, Favorskaya A, Pesnya E, Stetsyuk V. Modification of the Grid-Characteristic Method on Chimera

Meshes for 3D Problems of Railway Non-Destructive Testing. Lobachevskii Journal of Mathematics, 2023. 44(1):376-386.

16. Favorskaya A, Khokhlov N. Accounting for curved boundaries in rocks by using curvilinear and Chimera grids. Procedia Computer Science, 2021, 192:3787-3794.
17. Khokhlov N, Favorskaya A, Stetsyuk V, Mitskovets I. Grid-characteristic method using Chimera meshes for simulation of elastic waves scattering on geological fractured zones. Journal of Computational Physics, 2021, 446(1):110637.
18. Ivan A. Mitskovets. Application of Chimeric Meshes for Explicit Accounting for Inhomogeneities in Modeling the Propagation of Elastic Waves. *RENSIT: Radioelectronics. Nanosystems. Information Technologies,* 2023, 15(2): 185-192e. DOI: 10.17725/rensit.2023.15.185.
19. Favorskaya AV, Khokhlov N. Using Chimera Grids to Describe Boundaries of Complex Shape. In: Czarnowski, I., Howlett, R.J., Jain, L.C. (eds) Intelligent Decision Technologies. Smart Innovation, Systems and Technologies, 2022, 309. Springer, Singapore.